

## SYNTHESIS AND CHARACTERIZATION OF TENORITE (CuO) NANOPARTICLES FROM SMELTING FURNACE DUST (SFD)

E. Darezereshki<sup>a</sup>, F. Bakhtiari<sup>b,c,\*</sup>

<sup>a</sup>Energy & Environmental Engineering Research Center (EERC), Shahid Bahonar University of Kerman, Iran

<sup>b</sup>Mineral Industries Research Centre, Shahid Bahonar University of Kerman, Iran

<sup>c</sup>Department of Chemical Engineering, Faculty of Engineering, Shahid Bahonar University of Kerman, Iran

(Received 11 April 2012; accepted 27 June 2012)

### Abstract

Tenorite (CuO) nanoparticles were prepared from a dilute CuSO<sub>4</sub> solution. The solution was obtained by leaching (pH=1.5) of smelting furnace dust of Sarcheshmeh Copper Complex, Iran. The recovery of copper from the acidic sulphate solution was carried out by solvent extraction using Lix 984-N. Tenorite nanoparticles were synthesized by direct thermal decomposition of Langite [Cu<sub>4</sub>(OH)<sub>6</sub>SO<sub>4</sub>(H<sub>2</sub>O)<sub>2</sub>] as a precursor which was calcinated in air for 2 h at 750 °C. The Samples were characterized by X-ray diffraction, infrared spectroscopy, scanning electron microscopy, and transmission electron microscopy. The average diameter of the spherical pure CuO nanoparticles and their crystallite size were estimated to be 92 nm and 40 nm, respectively. The simplicity of the present method suggests its potential application at industrial scale as a cheap and convenient way to produce pure CuO nanoparticles from dilute CuSO<sub>4</sub> solutions obtained from leaching of smelting furnace dust.

**Keywords:** Copper Oxides; Nanoparticles; Leaching; Smelting furnace dust (SFD)

### 1. Introduction

Metal oxide nanoparticles have some special physical and chemical properties which make them superior to conventional metal oxide in many applications. In recent years, interests in developing nano-structured metal oxides with p-type semi-conductivity have been increased [1]. CuO nanoparticles are among the important inorganic semiconductors with a monoclinic structure and a direct band-gap value of 1.85 eV [2]. This material has potential in diverse technological applications as gas sensors [3-7], magnetic phase transmitters [8, 9], heterogeneous catalysts [6, 10-14], optical switches [3], solar energy transformer [4, 15, 16], lithium ion electrode materials [1, 6, 17, 18], nanofluids [19, 20] and field emitters [9, 21]. Several methods have been reported for synthesizing nanostructured copper oxide, namely the sol-gel [7, 11], and wet chemical methods [13, 22, 23], thermal oxidation of Cu substrates [3, 15], solvothermal [4, 9], microemulsion [14, 24], microwave irradiation [25], sonochemical [26], submerged arc [27], solid state reaction [28, 29], electrochemical [30], hydrothermal [31, 32] and

precipitation methods [19, 33, 34]. Thermal decomposition of precursors [1, 35-40] and co-precipitation [41] are also used to produce nanoparticles. Kida et al. [4] reported the preparation of stable copper oxide nanoparticle by alcoholthermal technique. A large amount of organic solvents, however, were required in the preparation process. Li and Chang [19] prepared a stable colloidal solution of copper (II) oxide in n-alkanes via oleate modifications. This method is too cumbersome and may not be appropriate for production of CuO nanoparticles in large scales. The microemulsion is a common procedure for the synthesis of 1D nanostructure. But this method is prone to a scattered distribution of reactants and the product would have a wide size distribution [14, 24]. Ranjbar et al. [26] presented a novel sonochemistry method to prepare CuO nanoparticles in organic solvents. The method needed expensive ultrasonic equipment, extreme conditions of reaction, and an excessive amount of organic solvents. Solid reactant structure and reaction thermodynamics are effective in the solid-state reaction condition, at ambient temperature [28]. Since, the fine reactant particles can react faster,

\* Corresponding author: Fereshteh@uk.ac.ir

crushing is very important for the production of CuO nanoparticles with solid-state reaction method which means greater operation cost. Well-dispersed CuO nanoparticles could be prepared by a simple quick-precipitation method [19, 33, 34]. But this procedure requires a surfactant or an organic solvent for dispersing and stability of the nanoparticles. Overall, most of the above mentioned methods need special conditions, expensive instruments or large amounts of chemicals.

Among different methods developed for the preparation of copper oxide nanoparticles, thermal decomposition is a new technique which is much cleaner, faster, and economical compared to common methods. This method involves the selection of a proper precursor and localized heating. Copper oxide nanoparticles can be prepared by the thermal decomposition of various copper salts including the oxalate, hydroxides and hydroxyl salts obtained from direct deposition and pyrolysis method [1, 35, 36]. Zhang and et al. [1] produced copper nanoparticles with the average diameter of 10 nm from the thermal decomposition of copper oxalate precursor. Copper (II) oxide nanoparticles may be synthesized by thermal decomposition of  $\text{CuCO}_3 \cdot \text{Cu}(\text{OH})_2$  [35, 36] or dehydration of  $\text{Cu}(\text{OH})_2$  [34]. CuO nanoparticles were also synthesized from the thermal decomposition of the precursors Brochantite  $\text{Cu}_4(\text{SO}_4)(\text{OH})_6$ , and Posnjakite  $\text{Cu}_4(\text{SO}_4)(\text{OH})_6 \cdot \text{H}_2\text{O}$  [37, 38]. However, few research papers [37, 38] have been published on the preparation of CuO nanoparticles by the thermal decomposition of copper sulfate.

The precursors used for the preparation of CuO nanoparticles are usually obtained from materials with high purity. In this paper a method is presented to produce high-purity CuO nanoparticles from dilute  $\text{CuSO}_4$  solutions. The solution was obtained from the leaching of smelting furnace dust (SFD). This novel method does not require expensive equipments, organic solvents or complex techniques and may produce the copper oxide in large amounts. This is the first report on the synthesis of CuO nanoparticles with high purity from industrial materials.

## 2. Materials and Methods

### 2.1. Materials

The raw material was a sample of smelters copper dust from the smelting factory of Sarcheshmeh Copper Complex, Iran. Samples were collected over a

seven-day period during the smelting process and mixed to obtain a representative sample. Chemical and mineral analysis of the dust showed that it contained 36% Cu and 22.2% Fe and major copper sulfide minerals in the dust were chalcocite 19%, chalcopyrite 2%, covellite 2% and bornite 3%. The acid soluble copper content of the dust was 13% [42-44].

Concentrated sulfuric acid was used for acid leaching. Lix984-N which is an equal mixture of 5 dodecylsalicylaldoxime (Lix860N-I) and 2-hydroxy-5-nonyl-acetophenone oxime (Lix84-I) with a proprietary diluent were used for solvent extraction to obtain dilute  $\text{CuSO}_4$  solutions.  $\text{Na}_2\text{CO}_3$ , distilled and de-ionized water were used in the synthesis process. All of the reagents used in the synthesis were of analytical grade purity.

### 2.2. Experimental

Experimental studies were carried out in the following three stages.

#### 2.2.1. Acid leaching

Acid leaching was carried out with a sulfuric acid solution (pH 1.5) and 10% (w/v) pulp density at room temperature. The pH was adjusted to 1.5 during the leaching by adding concentrated sulfuric acid. This led to the dissolution of about 80% of the acid soluble portion of copper after 3 h. Inductive Coupled Plasma (ICP-MS, Varian 715-ES) analysis of the leaching solution is shown in Table 1.

#### 2.2.2. Solvent extraction of copper sulfate solution

Dilute  $\text{CuSO}_4$  solutions were obtained from leaching solution by solvent extraction. The concentration of solvent extractor in organic phase (Lix984-N) was 8 percent. The rest of the organic phase was the proprietary diluent. 150 mL of the organic phase was added to 150 mL of leaching solution in a separating funnel. The mixture was shaken thoroughly for 1 minute. After separation of the two phases, the aqueous phase was put aside and solvent extraction was done on the organic phase again. A wash stage was carried out before next extraction to remove some impurities like Fe and to obtain pure  $\text{CuSO}_4$  solution. The organic phase was mixed with a solution containing  $3 \text{ g L}^{-1}$  Cu and  $15 \text{ g L}^{-1}$   $\text{H}_2\text{SO}_4$  and solvent extraction was done one time to

**Table 1.** ICP chemical composition of the obtained solution from acid leaching of dust (SFD).

Element	Cu	Fe	Ag	Mg	Mn	Mo	Pb	Sb
Concentration (mg L <sup>-1</sup> )	20925.4	6322.3	4.67	112.5	7.47	118.5	16.74	96.07

wash the organic phase. Then, an equal volume of sulfuric acid solution (200 g L<sup>-1</sup>) was added to the separating funnel which contained the washed organic phase. After mixing and separation of two phases, the organic phase was put aside and the aqueous phase which contained CuSO<sub>4</sub> was used for the synthesis of CuO nanoparticles. The chemical analysis of the aqueous phase is shown in Table 2.

with distilled water and absolute ethanol. The precipitate was then dried at 70°C for several hours. The thermal behavior of the precursor was studied with thermogravimetry (TG-DSC), (STA409PG instrument) under atmosphere flow. 35 mg of samples were placed in a platinum crucible on the pan of a microbalance and were heated with the heating rate of 10 °C/min in the temperature range of 25–900 °C.

**Table 2.** ICP chemical composition of the obtained solution from solvent extraction of leaching solution.

Element	Cu	Fe	Ag	Mg	Mn	Mo	Pb	Sb
Concentration (mg L <sup>-1</sup> )	12806.9	84.3	1.9	53.9	0.38	1.55	0.45	----

### 2.2.3. Synthesis of Copper Oxide nanoparticles

Langite [Cu<sub>4</sub>(OH)<sub>6</sub>SO<sub>4</sub>(H<sub>2</sub>O)<sub>2</sub>] was prepared by drop wise addition of 2 M Na<sub>2</sub>CO<sub>3</sub> solution to the 0.2 M (12806.9 mg L<sup>-1</sup>) CuSO<sub>4</sub> solution. The CuSO<sub>4</sub> solution was vigorously stirred at 55°C. The green precipitate was separated by filtration and washed

Some of the precursor was calcined in air in a muffle furnace at 750°C for 2 h. The pathway process which occurred in the preparation of product is shown in Fig. 1. The crystalline structure of the nanoparticles was characterized by X-Ray diffraction (XRD, PHILIPS, X'pert-MPD system) using Cu Kα (λ=1.54 Å) radiation. Infrared (IR) spectra were recorded on a Bruker tensor 27 Fourier Transform infrared (FTIR) spectrometer with RT-DLATGS detector, in the range of 400 to 4000 cm<sup>-1</sup> with a spectral resolution of 4 cm<sup>-1</sup> in transmittance mode. The KBr pellet technique was used for sample preparation using sample concentration 1 wt%. The morphology and average particle size of CuO nanoparticles were also determined with scanning electron microscopy (SEM, Tescan Vega-II) and transmission electron microscopy (TEM, PHILIPS CM20).

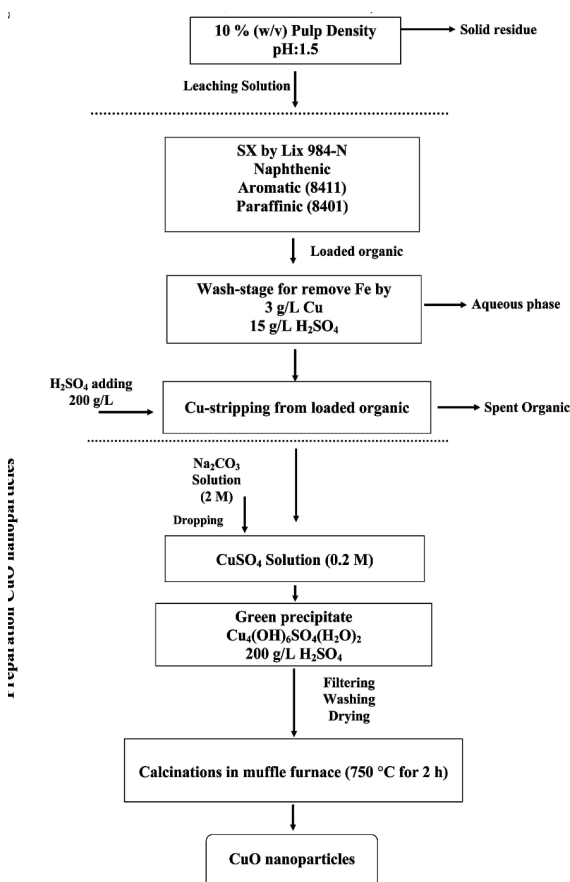


**Figure 1.** Working flow sheet of the process for recovery of copper from SFD and product CuO nanoparticles..

### 3. Results and discussion

The crystal structure and the phase purity of the precursor were characterized by XRD. As Fig. 2 shows almost all the diffraction peaks of the precursor could be indexed to langite [Cu<sub>4</sub>(OH)<sub>6</sub>SO<sub>4</sub>(H<sub>2</sub>O)<sub>2</sub>] with lattice constants of a = 7.137 Å, b = 6.031 Å, c = 11.217 Å, and Azurite [2CuCO<sub>3</sub>·Cu(OH)<sub>2</sub>] with lattice constants of a = 4.97 Å, b = 5.84 Å, c = 10.29 Å, which are in good agreement with the standard XRD data (JCPDS card No. 01-075-1258 and 00-011-0136). Moreover, the FTIR spectra provided information on the main phase of the produced precursor. Fig. 3a shows the FTIR spectrum of the Cu<sub>4</sub>(OH)<sub>6</sub>SO<sub>4</sub>(H<sub>2</sub>O)<sub>2</sub>. The absorption bands at 426, 487, 601, 987 and 1123 cm<sup>-1</sup> are attributed to sulfate groups (SO<sub>4</sub><sup>2-</sup>) [37]. The peaks at 735, 784, 878, 945 and 987 cm<sup>-1</sup> are attributed to Cu-OH vibrations [45, 46]. Low absorption are also visible in the region of carbonate vibrations (1371 cm<sup>-1</sup> and 1480 cm<sup>-1</sup>), but does not allow identification of the compound. So, Langite [Cu<sub>4</sub>(OH)<sub>6</sub>SO<sub>4</sub>(H<sub>2</sub>O)<sub>2</sub>] is detected, in agreement with the X-Ray diffraction. The absorption bands visible on the spectra around 1631 cm<sup>-1</sup> are

characteristic of vibrations in structural water molecules and the band at  $3421\text{ cm}^{-1}$  is attributed to -OH-stretching [47]. Finally, the tiny dip in the spectra at  $2364\text{ cm}^{-1}$  is due to atmospheric  $\text{CO}_2$  [37, 47].

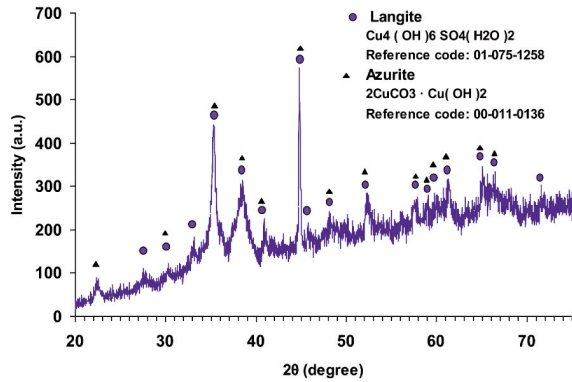


Figure 2. X-ray patterns of the Langite  $[\text{Cu}_4(\text{OH})_6\text{SO}_4(\text{H}_2\text{O})_2]$ .

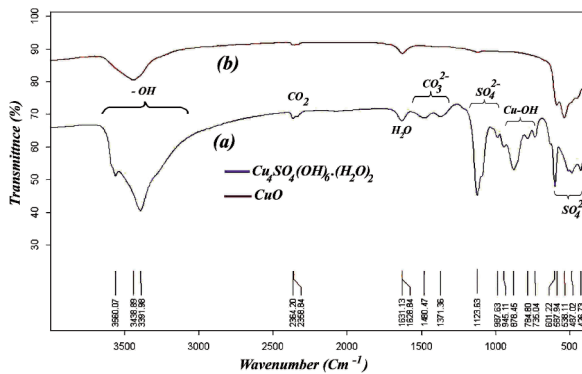
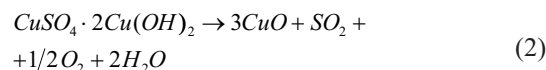
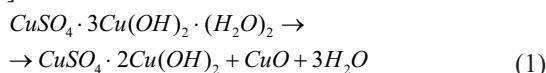


Figure 3. (a) FT-infrared spectra of the precursor  $(\text{Cu}_4(\text{OH})_6\text{SO}_4(\text{H}_2\text{O})_2)$  and (b) CuO nanoparticles performed by 250 mg KBr.

Fig. 4 shows a typical TG-DSC analysis for  $\text{Cu}_4(\text{OH})_6\text{SO}_4(\text{H}_2\text{O})_2$ . Three endothermic ( $380.4\text{ }^\circ\text{C}$ ;  $669\text{ }^\circ\text{C}$ ;  $884.1\text{ }^\circ\text{C}$ ) and an exothermic peak ( $520.3\text{ }^\circ\text{C}$ ) were observed. The three endothermic peaks correspond to the dehydroxylation of the basal hydroxide layers ( $380.4\text{ }^\circ\text{C}$ ) (Eq. (1)), the decomposition of sulfate groups (Eq. (2)), and the reduction of CuO to  $\text{Cu}_2\text{O}$  (Eqs. (3)), respectively.

The exothermic peak corresponds to the crystallization of the amorphous dehydrated product, followed by the endothermic desulfurization reaction [37].



The precursor  $[\text{Cu}_4(\text{SO}_4)(\text{OH})_6(\text{H}_2\text{O})_2]$  readily converts to CuO (JCPDS card No. 01-074-1021,  $a=4.6530\text{ \AA}$ ,  $b=3.4100\text{ \AA}$ ,  $c=5.1080\text{ \AA}$ , and  $\beta=99.48^\circ$ ) when heated at  $750\text{ }^\circ\text{C}$  for 2 h (Fig. 5). The products consist of pure phases. The TEM images did not show any specific defects in the nanostructure, so the crystalline size was estimated from XRD diffraction peaks using Scherrer's formula (Table 3). Average crystallite sizes were estimated using the Scherrer formula applied to the line broadening obtained from the major reflections and was found to be around 40 nm.

Fig. 3b shows the FTIR spectrum of the CuO nanoparticles. The absorption peak at  $538$  and  $587\text{ cm}^{-1}$  is attributed to  $\text{Cu}(\text{II})\text{-O}$  [30], which is in agreement with the results of XRD. The SEM images of precursor and CuO nanoparticles are shown in Fig. 6 and Fig. 7, respectively. The morphology of the precursor  $[\text{Cu}_4(\text{OH})_6\text{SO}_4(\text{H}_2\text{O})_2]$  and nano-sized CuO nanoparticles were flower-like shape and spherical, respectively. Some of the nanoparticles became agglomerated and sintered during heating. The TEM image of CuO nanoparticles is shown in Fig. 8a and b. TEM observations showed that the CuO nanoparticles have a wide size distribution with the average diameter of 92 nm (Fig. 8c).

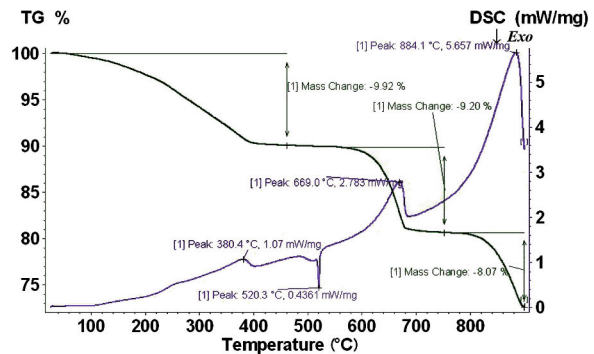


Figure 4. TGA-DSC curves of the precursor  $(\text{Cu}_4(\text{OH})_6\text{SO}_4(\text{H}_2\text{O})_2)$  from 35 to  $900\text{ }^\circ\text{C}$ .

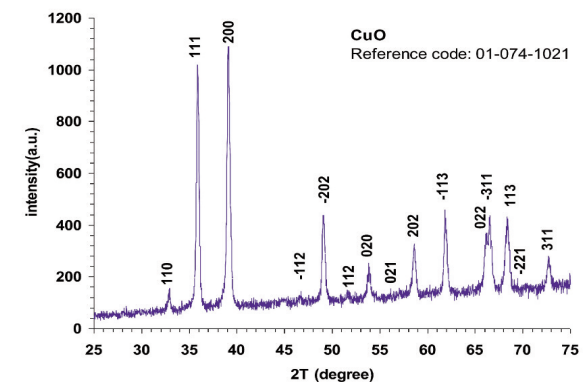
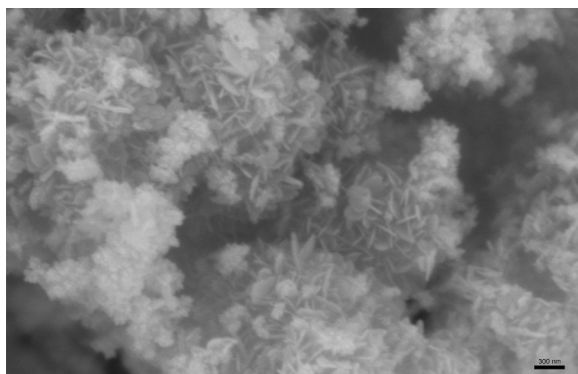


Figure 5. X-ray patterns of CuO nanoparticles.

**Table 3.** Representative X-ray powder diffraction data and the size of crystallites estimated from the diffraction peaks.

h	k	l	d <sub>cal.</sub>	d <sub>meas.</sub>	Crystallite size (Å°)
1	1	0	2.73716	2.7335	528
1	1	1	2.31177	2.33294	424
2	0	0	2.29473	2.30454	476
-1	1	2	1.95156	1.94868	183
-2	0	2	1.85535	1.85649	493
1	1	2	1.76902	1.76718	144
0	2	0	1.705	1.7026	283
0	2	1	1.61503	1.61785	861
2	0	2	1.57238	1.57529	331
-1	1	3	1.49857	1.49995	337
0	2	2	1.41199	1.41108	282
-3	1	1	1.40036	1.40564	604
1	1	3	1.37261	1.37178	271
-2	2	1	1.35482	1.35373	293
3	1	1	1.29595	1.29933	257



**Figure 6.** SEM image of the Precursor  $[Cu_4(OH)_6SO_4(H_2O)_2]$ .

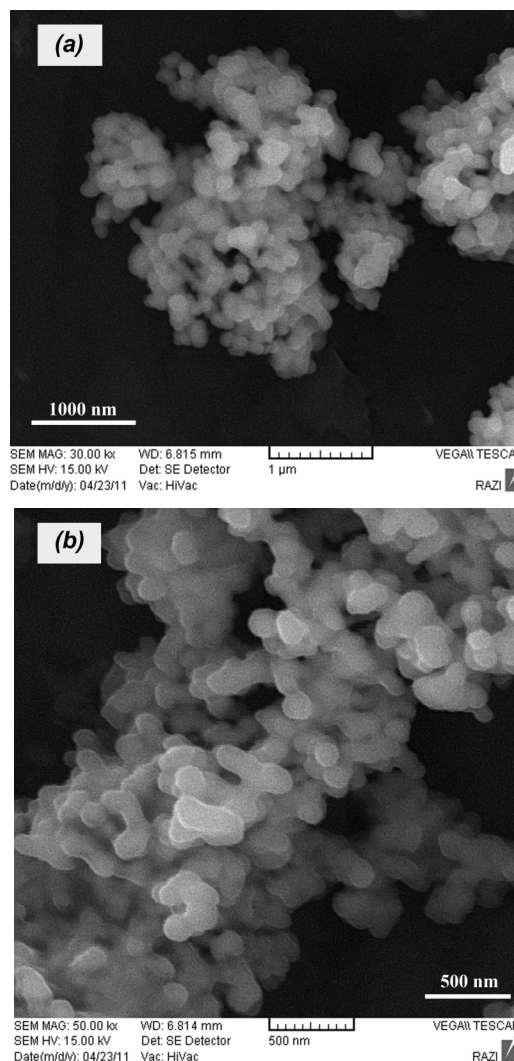


**Figure 7.** (a, b) SEM images of the CuO nanoparticles synthesized by direct thermal decomposition of Langite at 750 °C for 1 h ((a) 30,000× and (b) 50,000× magnification).

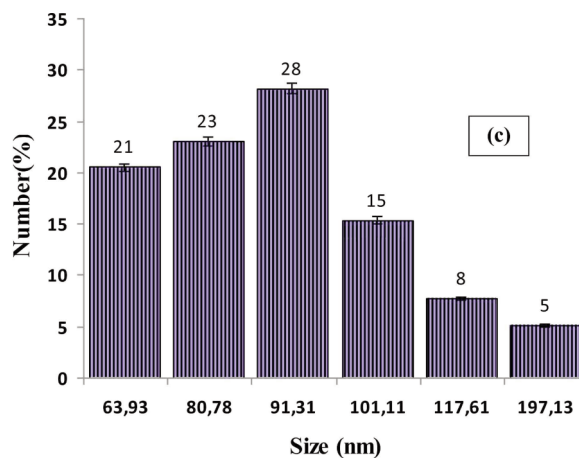
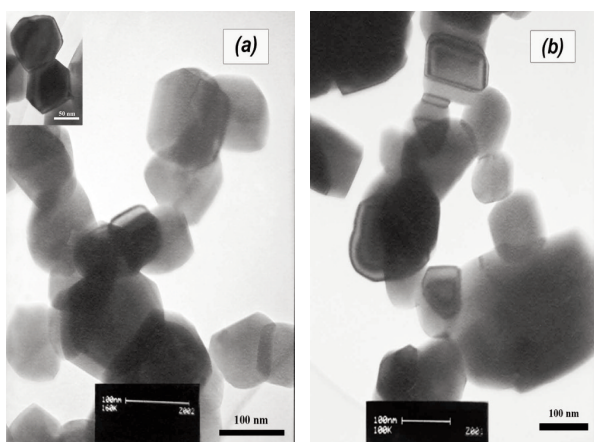


**Figure 8.** (a, b) TEM images and (c) particle size distribution of the CuO nanoparticles.

#### 4. Conclusion

This study was shown that CuO nanoparticles can be produced by direct thermal decomposition method using Langite  $[\text{Cu}_4(\text{OH})_6\text{SO}_4(\text{H}_2\text{O})_2]$  as a precursor. The precursor was synthesized from  $\text{CuSO}_4$  solution obtained from leaching of copper smelting dust with sulfuric acid. Pure CuO nanoparticle with the approximate size of 92 nm was prepared by calcination of the precursor at 750 °C for 2 h. The presented method does not require organic solvents, surfactants, expensive raw materials, and it is not time consuming. So, this method could be used for the synthesis of tenorite nanoparticles from  $\text{CuSO}_4$  solution which may be obtained from leaching and bioleaching of copper dust. This might be applied at industrial scale as a cheap and convenient approach in the production of pure tenorite nanoparticles.

#### Acknowledgements

*The authors would like to express their grateful Dr. Mohammad Hassan Fazaalipoor for his comments in the preparation of the manuscript.*

#### References

- [1] X. Zhang, D. Zhang, X. Ni, H. Zheng, Solid-State Electron., 52 (2) (2008) 245-248.
- [2] M. A. Rafea, N. Roushdy, J. Phys. D: Appl. Phys., 42 (1) (2009) 015413.
- [3] B. J. Hansen, N. Kouklin, G. Lu, I. K. Lin, J. Chen, X. Zhang, J. Phys. Chem. C, 114 (6) (2010) 2440-2447.
- [4] T. Kida, T. Oka, M. Nagano, Y. Ishiwata, X. G. Zheng, J. Am. Ceram. Soc., 90 (1) (2007) 107-110.
- [5] J. Zhang, J. Liu, Q. Peng, X. Wang, Y. Li, Chem. Mater., 18 (4) (2006) 867-871.
- [6] C. Lu, L. Qi, J. Yang, D. Zhang, N. Wu, J. Ma, J. Phys. Chem. B, 108 (46) (2004) 17825-17831.
- [7] N. Topnani, S. Kushwaha, T. Athar, Int. J. Green Nanotechnol. Mater. Sci. Eng., 1 (2009) M67-M73.
- [8] Y. P. Sukhorukov, N. N. Loshkareva, A. A. Samokhvalov, S. V. Naumov, A. S. Moskvina, A. S. Ovchinnikov, J. Magn. Magn. Mater., 183 (3) (1998) 356-358.
- [9] M. A. Dar, Y. S. Kim, W. B. Kim, J. M. Sohn, H. S. Shin, Appl. Surf. Sci., 254 (22) (2008) 7477-7481.
- [10] J. B. Wang, D. H. Tsai, T. J. Huang, J. Catal., 208 (2) (2002) 370-380.
- [11] C. L. Carnes, K. J. Klabunde, J. Mol. Catal. A: Chem., 194 (1-2) (2003) 227-236.
- [12] J. Wang, S. He, Z. Li, X. Jing, M. Zhang, Mater. Sci. Poland, 27 (2) (2009) 501-507.
- [13] L. M. Zhang, W. C. Lu, Y. L. Feng, J. P. Ni, Y. Lu, X. F. Shang, Acta Phys. Chim. Sin., 24 (12) (2008) 2257-2262.
- [14] C. Li, Y. Yin, H. Hou, N. Fan, F. Yuan, Y. Shi, Q. Meng, Solid State Commun., 150 (13-14) (2010) 585-589.
- [15] T. Yu, X. Zhao, Z. X. Shen, Y. H. Wu, W. H. Su, J. Cryst. Growth, 268 (3-4) (2004) 590-595.
- [16] S. Anandan, X. Wen, S. Yang, Mater. Chem. Phys., 93 (1) (2005) 35-40.
- [17] X. P. Gao, J. L. Bao, G. L. Pan, H. Y. Zhu, P. X. Huang, F. Wu, D. Y. Song, J. Phys. Chem. B, 108 (18) (2004) 5547-5551.
- [18] X. Zhang, D. Zhang, X. Ni, J. Song, H. Zheng, J. Nanopart. Res., 10 (5) (2008) 839-844.
- [19] C. C. Li, M. H. Chang, Mater. Lett., 58 (30) (2004) 3903-3907.
- [20] M. H. Chang, H. S. Liu, C. Y. Tai, Powder Technol., 207 (1-3) (2011) 378-386.
- [21] C. T. Hsieh, J. M. Chen, H. H. Lin, H. C. Shih, Appl. Phys. Lett., 83 (16) (2003) 3383-3385.
- [22] Y. Kobayashi, T. Maeda, K. Watanabe, K. Ihara, Y. Yasuda, T. Morita, J. Nanopart. Res., 13 (10) (2011) 5365-5372.
- [23] L. Sun, Z. Zhang, Z. Wang, Z. Wu, H. Dang, Mater. Res. Bull., 40 (6) (2005) 1024-1027.
- [24] D. Han, H. Yang, C. Zhu, F. Wang, Powder Technol., 185 (3) (2008) 286-290.
- [25] P. J. Cai, M. Shi, Adv. Mater. Res., 92 (2010), 117-123.
- [26] R. Ranjbar-Karimi, A. R. Bazmandegan-Shamili, A. R. Aslani, K. Kaviani, Physica B, 405 (15) (2010) 3096-3100.
- [27] C. H. Lo, T. T. Tsung, L. C. Chen, C. H. Su, H. M. Lin, J. Nanopart. Res., 7 (2-3) (2005) 313-320.
- [28] W. Jisen, Y. Jinkai, S. Jinquan, B. Ying, Mater. Design, 25 (7) (2004) 625-629.
- [29] W. Wang, Y. Zhan, X. Liu, C. Zheng, G. Wang, Mater. Res. Bull., 37 (14) (2002) 1093-1100.
- [30] N. Liu, D. Wu, H. Wu, C. Liu, F. Luo, Mater. Chem. Phys., 107 (2) (2008) 511-517.
- [31] Q. Liu, H. Liu, Y. Liang, Z. Xu, G. Yin, Mater. Res. Bull., 41 (4) (2006) 697-702.
- [32] W. Jia, E. Reitz, P. Shimpi, E. G. Rodriguez, P.X. Gao, Y. Lei, Mater. Res. Bull., 44 (8) (2009) 1681-1686.
- [33] J. Zhu, D. Li, H. Chen, X. Yang, L. Lu, X. Wang, Mater. Lett., 58 (26) (2004) 3324-3327.
- [34] R. Wu, Z. Ma, Z. Gub, Y. Yang, J. Alloy. Compd., 504 (1) (2010) 45-49.
- [35] H. Fan, L. Yang, W. Hua, X. Wu, Z. Wu, S. Xie, B. Zou, Nanotechnology, 15 (1) (2004) 37-42.
- [36] C. L. Zhu, C. N. Chen, L. Y. Hao, Y. Hu, Z. Y. Chen, Solid State Commun., 130 (10) (2004) 681-686.
- [37] F. Bakhtiari, E. Darezereshki, Mater. Lett., 65 (2011) 171-174.
- [38] E. Darezereshki, F. Bakhtiari, J. Min. Metall. Sect. B-Metall., 47 (1) B (2011) 73-78.
- [39] A. G. Nasibulin, P. P. Ahonen, O. Richard, E. I. Kauppinen, I. S. Altman, J. Nanopart. Res., 3 (5-6) (2001) 385-400.
- [40] C. Xu, Y. Liu, G. Xu, G. Wang, Mater. Res. Bull., 37 (14) (2002) 2365-2372.
- [41] R. Ahmadi, H. R. Madaah Hosseini, A. Masoudi, J. Min. Metall. Sect. B-Metall., 47 (2) B (2011) 211-218.
- [42] F. Bakhtiari, M. Zivdar, H. Atashi, S. A. Seyed Bagheri, Hydrometallurgy, 90 (1) (2008) 40-45.
- [43] F. Bakhtiari, H. Atashi, M. Zivdar, S. A. Seyed Bagheri, Int. J. Miner. Process., 86 (1) (2008) 50-57.
- [44] F. Bakhtiari, H. Atashi, M. Zivdar, S. A. Seyedbagheri, M.H. Fazaalipoor, J. Ind. Eng. Chem., 17 (1) (2011) 29-35.
- [45] J. Y. Malvault, J. Lopitiaux, D. Delahaye, M. Lenglet, J. Appl. Electrochem., 25 (9) (1995) 841-845.
- [46] C. H. Hsieh, S. L. Lo, C. Y. Hu, K. Shih, W. S. Kuan, C. L. Chen, Chemosphere, 71 (9) (2008) 1693-1700.
- [47] E. Darezereshki, M. Alizadeh, F. Bakhtiari, M. Schaffie, M. Ranjbar, Appl. Clay Sci., 54 (1) (2011) 107-111.